Short Communication

Mouhamadou Birame Diop*, Libasse Diop, Laurent Plasseraud* and Hélène Cattey

Triorganotin carboxylates — synthesis and crystal structure of 2-methyl-1*H*-imidazol-3-ium catena-O,O'-oxalatotriphenylstannate

DOI 10.1515/mgmc-2016-0016 Received April 12, 2016; accepted May 30, 2016; previously published online June 29, 2016

Abstract: The reaction of bis(2-methyl-1*H*-imidazol-3-ium) oxalate, $[C_{\lambda}H_{\gamma}N_{\gamma}]_{\gamma}[C_{\gamma}O_{\lambda}]$, and bis(triphenyltin) oxalate, $[(Ph_sSn)_s(C_sO_s)]$, in methanol at room temperature yielded the formation of 2-methyl-1H-imidazol-3-ium catena-0,0'oxalatotriphenylstannate, $[C_{A}H_{7}N_{3}][Ph_{3}Sn(C_{3}O_{A})]$ (1), which crystallizes in the monoclinic space group P2/c with Z=8, a=16.9334(14) Å, b=17.3251(14) Å, c=14.5114(10) Å, β =90.590(2)°, and V=4257.0(6) Å³. The oxalate ligand of 1 displays a bridging coordination mode and thus links two SnPh, moieties through an axial coordination leading to the propagation of infinite polymeric chains along the c axis. All Sn(IV) atoms exhibit a trigonal bipyramid geometry. The negative charge of $[Ph_sSn(C_sO_a)]^-$ moieties is compensated by the presence of surrounding noncoordinating 2-methyl-1H-imidazol-3-ium cations. From a supramolecular point of view, the Sn-based chains are connected to one another through N-H···O hydrogen bond interactions involving oxalate ligands of distinct strands and doubly by the $[C_{\nu}H_{\nu}N_{\nu}]^{+}$ cations. The topology of the resulting crystal packing can be described as a two-dimensional layer network.

Keywords: organotin (IV) carboxylates; oxalate ligand; self-assembly; triphenyltin; X-ray crystallography.

F-21000 Dijon, France

Introduction

Organotin (IV) carboxylates are an important class of organotin compounds. They were reported in the literature from a long time and have been widely studied since (Davies, 2004; Davies et al., 2008). Because of its catalytic properties (Meneghetti and Meneghetti, 2015) and biological activity (Gielen et al., 2005; Hadjikakou and Hadjiliadis, 2009), studies on organotin (IV) carboxylates are continuing and still arouse a great interest. Thus, recent studies have been published regarding the catalytic synthesis of aliphatic urethanes (Devendra et al., 2015) as well as the potential anticancer activity of organotin (IV) carboxylates (Amir et al., 2014; Sirajuddin et al., 2014). Lately, the fungicidal activity of triorganotin (IV) 1-methyl-1H-imidazole-4-carboxylates was also reported (Mao et al., 2015). From a structural point of view, numerous papers and review articles have been reported describing the different modes of coordination of carboxylates to organotin (IV) moieties and showing a great diversity of molecular structures (Tiekink, 1991; Chandrasekhar et al., 2002). In this area, several contributions have been reported by the Senegalese group, focusing in particular on the isolation of new oxalates of stannates (IV) (Gueve et al., 2014; Diop et al., 2016). A particular attention was given to the coordination of triorganotin (IV) derivatives (Diop et al., 1997, 2003; Gueye et al., 2011, 2012; Sow et al., 2012). In the field of crystal engineering and supramolecular coordination chemistry, organotin carboxylates can also be viewed as suitable building blocks (Tiekink, 2006). Indeed, in addition to the tin hypervalency, carboxylic acid-based ligands are considered as appropriate connectors to promote the formation of multidirectional architectures (Ivasenko and Perepichka, 2011). Furthermore, the cocrystallization of nitrogen organic compounds significantly increases the potential of linkage and the diversity of topology, via the formation of ammonium cations and the creation of new hydrogen-bonded networks. Imidazolium derivatives

^{*}Corresponding authors: Mouhamadou Birame Diop, Laboratoire de Chimie Minérale et Analytique, Département de Chimie, Faculté des Sciences et Techniques, Université Cheikh Anta Diop, Dakar, Senegal, e-mail: mouhamadoubdiop@gmail.com; and Laurent Plasseraud, ICMUB UMR CNRS 6302, Université de Bourgogne Franche-Comté, Faculté des Sciences, 9 avenue Alain Savary, F-21000 Dijon, France, e-mail: laurent.plasseraud@u-bourgogne.fr Libasse Diop: Laboratoire de Chimie Minérale et Analytique, Département de Chimie, Faculté des Sciences et Techniques, Université Cheikh Anta Diop, Dakar, Senegal Hélène Cattey: ICMUB UMR CNRS 6302, Université de Bourgogne Franche-Comté, Faculté des Sciences, 9 avenue Alain Savary,

are especially well suited for such approach. In 2010, Callear et al. (2010) focused on the crystal packing effects of the methylation of different atoms around the imidazole ring. In this context, we recently started to investigate the contribution of 2-methyl-1*H*-imidazol-3-ium in the presence of tin oxalates revealing, in particular, an interesting 3,5T1 topological network (Diop et al., 2015). Continuing our investigations, we report herein on the synthesis and characterization of the 2-methyl-1*H*-imidazol-3-ium catena-*O*,*O*′-oxalatotriphenylstannate (1), which is organized in the solid state into the polymeric chains connected by 2-methyl-1*H*-imidazol-3-ium cations (Scheme 1).

Compound 1 was synthesized by reacting methanolic solutions of bis(triphenyltin) oxalate, [(Ph₂Sn)₂(C₂O₄)], and bis(2-methyl-1H-imidazol-3-ium) oxalate, $[C_6H_7N_3]_2[C_2O_6]$ (Equation 1). Colorless crystals, obtained by a slow evaporation of the solvent at room temperature, were first studied by ATR-FTIR spectroscopy (Figure S1). The strong bands located at 1616 and 1594 cm⁻¹ and 1424 cm⁻¹ can be assigned to $v_{sc}(COO^{-})$ and $v_{c}(COO^{-})$ stretching vibrations of carboxylate groups, respectively. Those observed at 1286 and 1245 cm⁻¹, both of comparable intensity, are attributed to ν (C-COO⁻) vibration bands. Characteristic absorptions of phenyl and imidazole rings are positioned at 732 and 698 cm⁻¹ and 758 and 662 cm⁻¹, respectively, corresponding to $\delta({\rm C_{sp2}}$ -H) and $\delta({\rm C=C})$ elongations. The experimental CHN elemental analysis corroborates the formula of 1 but requires the addition of a half molecule of water to match fully with the theoretical values. Although not detected by XRD, the hygroscopic character of 1 can be explained by its ionic nature.

The molecular structure of **1** was finally elucidated by an X-ray crystallographic analysis performed on suitable

Scheme 1: Molecular representation of the polymeric structure of **1**.

crystals. Crystallographic data and refinement details are summarized in Table 1. An ORTEP view of the asymmetric unit is shown in Figure 1. The unit cell comprises two distinct entities. Selected bond lengths (Å) and angles (°) are presented in Table 2. The primary structure of 1 can be considered as a coordination polymer chain wherein $[Ph_3Sn(C_3O_4)]$ constitutes the repeating pattern. Oxalates exhibit a bidentate bridging coordination, trans-linking two distinct Ph, Sn moieties and thus promoting the extension of the chains running along the *c* axis. The geometry around the tin atoms corresponds to a distorted trigonal bipyramid (TBP). The equatorial positions are occupied by the three phenyl groups [C1-Sn1=2.128(2) Å, C7-Sn1= 2.138(2) Å, and C13-Sn1=2.152(2) Å; C21-Sn2=2.1188(19) Å, C27-Sn2=2.129(2) Å, and C33-Sn2=2.135(2) Å]. The sums of the angles at tin with the ipso-carbon atoms [C1-Sn1-C7=115.02(8)°, C7-Sn1-C13=132.35(7)°, C13-Sn1- $C1=112.26(8)^{\circ}$; C21-Sn2-C33=115.09(8)°, C33-Sn2-C27=127.89(7)°, C27-Sn2-C21=117.01(8)°] are 359.63° and 359.99°, respectively, indicating an almost perfect planarity. The variations recorded for the Sn-C bonds and C-Sn-C angles reflect the distortion of the TBP environment. The apical positions are occupied by two oxygen atoms of two distinct oxalate ligands [Sn1-O1 2.2190(14) Å and Sn1-O4 2.2164(13) Å; Sn2-O5 2.2574(13) Å and Sn2-O8 2.2992(13) Å]. These values are in the range of those already observed for polymeric oxalatotriphenylstannates and previously reported in the literature (Ng and Kumar Das, 1993; Ng et al., 1994). The corresponding axial angles O1-Sn1-O4 and O5-Sn2-O8 equal to 173.82(5)° and 174.01(5)°, respectively, indicating a slight deviation from linearity. In the unit cell, oxalate ligands exhibit two distinct conformations: one antiperiplanar [O1-C19-C20-O4=170.6(2)°] and one synclinal [05-C39-C40-08=57.8(2)°], leading to a differentiation between the chains. This structural feature is also supported by the infrared spectrum, which exhibits two distinct $v_{\infty}(COO^{-1})$ absorptions at 1616 and 1594 cm⁻¹ (Figure S1). The Sn1···O2 and Sn2···O6 distances measure 3.3717(15) and 3.2579(14) Å, respectively, but cannot be considered as significant interactions (Tiekink, 1991). For comparison, in the bis(dicyclohexylammonium) trisoxalatotetrakis(tri-n-butylstannate), which describes a similar tin environment, this distance is 3.043(3) Å (Ng et al., 1990). Two columns are then observed according to the c axis, one composed by the Sn1 antiperiplanar chain and the second with the Sn2 synclinal chain. Furthermore, two separate types of lengths are observed for C-O bonds [C19-O1=1.271(2) Å, C20-O4=1.277(2) Å, C39-O5=1.280(2) Å, C40-O8=1.302(2) Å; C19-O2=1.235(2) Å, C20-O3=1.236(2) Å, C39-O6=1.238(2) Å, C40-O7=1.217(2) Å], thus distinguishing single- and double-bond character, respectively. The

Table 1: Crystal data and structure refinement of 1.

Formula	$0.5(C_{40}H_{30}O_8Sn_2)\cdot C_4H_7N_2$	
Formula weight (g·mol¹)	521.12	
Temperature	100 K	
Crystal system	Monoclinic	
Space group	$P2_{1}/c$	
Unit cell dimensions		
a (Å)	16.9334(14)	
b (Å)	17.3251(14)	
c (Å)	14.5114(10)	
α (°)	90	
β (°)	90.590(2)	
γ (°)	90	
Volume	4257.0(6) Å ³	
Z	8	
Density (calculated)	1.626 g⋅cm ⁻³	
Absorption coefficient	1.234 mm ⁻¹	
F(000)	2096	
Crystal size (mm)	$0.25 \times 0.20 \times 0.08$	
heta Range for data collection	2.985-27.540°	
Index ranges	$-22 \le h \le 22, -22 \le k \le 22,$	
	-17≤ <i>l</i> ≤18	
Reflections collected	163580	
Independent reflections	9799 [R(int)=0.0628]	
Completeness to $\theta_{ exttt{max}}$	99.8%	
Refinement method	Full-matrix least-squares on F^2	
Data/restraints/parameters	9799/0/561	
Goodness-of-fit ^c on F ²	1.056	
Final R indices $[I>2\sigma(I)]$	$R_1^{a}=0.0241$, $wR_2^{b}=0.0474$	
R indices (all data)	$R_1^a = 0.0357, wR_2^b = 0.0512$	
Largest difference peak/hole (e/ų) 1.227/-0.487		
CCDC number	1473073	

 $^{{}^{}a}R1=\Sigma(||F_{0}|-|F_{c}||)/\Sigma|F_{0}|.$ $^{b}wR2 = [\Sigma w(F_{0}^{2}-F_{0}^{2})^{2}/\Sigma[w(F_{0}^{2})^{2}]^{1/2}; \text{ where } w=1/2$ $[\sigma^2(F_a^2)+4.6826P+(0.0194P)^2]$, where $P=(\text{Max}(F_a^2,0)+2*F_a^2)/3$. ^cGoodness of fit= $\left[\sum w(F_0^2-F_0^2)^2/(N_0-N_0)\right]^{1/2}$.

negative charge of each [Ph,Sn(C,O,)] moieties is compensated by the presence of a 2-methyl-1H-imidazol-3-ium cation, positioned along the chains but noncoordinated to atoms of the chain. From a supramolecular point of view, each 2-methyl-1*H*-imidazol-3-ium cation exhibits two N-H···O hydrogen bond interactions with two oxygen atoms of oxalate ligands of two distinct strands [N1-H1···O2= 2.778(2) Å and N2-H2···O8=2.903(2) Å; N3-H3···O3=2.762(2) Å and N4-H4···O6=2.695(2) Å] along the a axis. In the past, similar topologies have been observed in the crystal lattices of the bis(dicyclohexylammonium) trisoxalatotetrakis(trin-butylstannate) (Ng et al., 1990) and of diorganoammonium oxalatotrimethylstannates, [R₂NH₂][Me₂Sn(C₂O₄)] (R=i-Bu, cyclohexyl) (Sow et al., 2012). 2-Methyl-1H-imidazol-3-ium cations are positioned perpendicularly to the axis of the tin-based strands and intercalated between the Ph₃Sn groups. The resulting supramolecular arrangement is depicted in Figure 2.

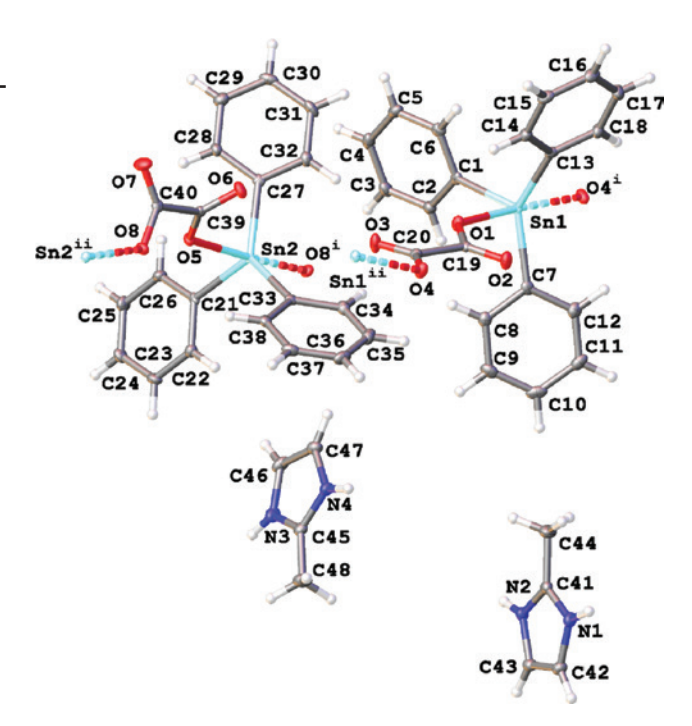


Figure 1: Molecular structure of 1 (asymmetric unit) showing 50% probability ellipsoids and the crystallographic numbering scheme (ORTEP view).

Color code: tin, turquoise; nitrogen, blue; oxygen, red; carbon, gray. Symmetry transformations used to generate equivalent atoms: (i) +x, 0.5-y, 0.5+z; (ii) +x, 0.5-y, -0.5+z.

We also sought to characterize 1 in solution by conducting in particular multinuclear NMR measurements. However, whatever the nature of the solvent used (chlorinated organic solvents, aromatics, and alcohols), we have not been able to record its ¹¹⁹Sn NMR fingerprint. Referring to the previous literature on oxalatotriphenylstannates (Ng and Kumar Das, 1993; Ng et al., 1994), we also found that this type of data was not available, leading us to assume that the polymeric nature of these derivatives strongly prevents their solubilization. Finally, the ¹H spectrum was obtained in CD₂OD (solvent used for crystallization). It highlights the characteristic signals of the 2-methyl-1H-imidazol-3-ium cation and phenyl groups and confirms the 1:3 ratio, respectively (Figure S2).

Experimental

General

2-Methylimidazole (C, H, N, 99% purity), oxalic acid dihydrate (HO,CCO,H-2H,O, 99% purity), and triphenyltin hydroxide (SnPh,OH, 95% purity) were purchased from Sigma-Aldrich (Steinheim am Albuch, Germany) and were used without any further purification. Infrared spectra were recorded on a Bruker Vector 22 spectrometer (Wissembourg, France) equipped with a Specac Golden Gate™ ATR

Table 2: Selected bond distances (Å) and angles (°) for **1**.

Sn1-01	2.2190(14)	Sn2-05	2.2574(13)
Sn1-04i	2.2164(13)	Sn2-08i	2.2992(13)
Sn102	3.3717(15)	Sn206	3.2579(14)
Sn1-C1	2.128(2)	Sn2-C21	2.1188(19)
Sn1-C7	2.138(2)	Sn2-C27	2.129(2)
Sn1-C13	2.152(2)	Sn2-C33	2.135(2)
01-C19	1.271(2)	05-C39	1.280(2)
02-019	1.235(2)	06-039	1.238(2)
03-020	1.236(2)	07-040	1.217(2)
04-Sn1 ⁱⁱ	2.2165(13)	08-Sn2 ⁱⁱ	2.2992(13)
04-C20	1.277(2)	08-C40	1.302(2)
Sn2-C2	1.396(3)		
04 ⁱ -Sn1-01	173.82(5)	C21-Sn2-C27	117.01(8)
C1-Sn1-O1	83.92(6)	C21-Sn2-C33	115.09(8)
C1-Sn1-04i	102.25(6)	C27-Sn2-O5	92.02(6)
C1-Sn1-C7	115.02(8)	C27-Sn2-08i	84.16(6)
C1-Sn1-C13	112.26(8)	C27-Sn2-C33	127.89(7)
C7-Sn1-O1	88.12(7)	C33-Sn2-O5	91.39(6)
C7-Sn1-04i	89.39(7)	C33-Sn2-08i	94.60(6)
C7-Sn1-C13	132.35(7)	C39-O5-Sn2	119.71(12)
C13-Sn1-O4i	86.21(6)	C40-08-Sn2ii	124.80(12)
C19-O1-Sn1	124.44(12)	C22-C21-Sn2	119.24(14)
C20-04-Sn1 ⁱⁱ	113.50(12)	C26-C21-Sn2	122.11(15)
C2-C1-Sn1	121.70(15)	C28-C27-Sn2	120.30(15)
C6-C1-Sn1	119.41(15)	C32-C27-Sn2	121.59(15)
C8-C7-Sn1	119.06(15)	C34-C33-Sn2	122.74(15)
C18-C13-Sn1	122.14(15)	C38-C33-Sn2	118.99(15)
01-C19-C20	112.66(17)	05-C39-C40	116.31(17)
02-C19-O1	126.65(18)	06-C39-O5	125.20(18)
02-C19-C20	120.67(17)	06-C39-C40	118.49(17)
03-C20-O4	125.38(18)	07-C40-08	127.23(19)
03-C20-C19	118.74(17)	07-C40-C39	119.34(18)
04-C20-C19	115.82(17)	08-C40-C39	113.41(17)
05-Sn2-08i	174.01(5)		
C21-Sn2-O5	86.78(6)		
C21-Sn2-08i	90.84(6)		

Symmetry transformations used to generate equivalent atoms: $^{i}+x$. $^{1}/_{2}-y$. $^{1}/_{2}+z$; $^{ii}+x$. $^{1}/_{2}-y$. $^{-1}/_{2}+z$.

device. ¹H NMR spectra were recorded at 300 K in CH₃OD on a Bruker Avance 300 spectrometer. Measurements of melting point were recorded using an Electrothermal 9100 capillary melting point apparatus. Elemental analyses were performed at the Institut de Chimie Moléculaire (Université de Bourgogne Franche-Comté, Dijon-France) using a Thermo Electron CHNS/O Flash EA 112 Series analyzer.

Synthesis of $[C_nH_1N_2][Ph_2Sn(C_2O_2)]$

Beforehand, bis(2-methyl-1H-imidazol-3-ium) oxalate, $[C_4H_7N_2]_2[C_2O_4]$, was prepared by reacting aqueous solutions of methyl-2-imidazole (1.000 g, 12.195 mmol) and oxalic acid dihydrate (0.769 g, 6.097 mmol). In parallel, bis(triphenyltin) oxalate, $[(SnPh_3)_2(C_2O_4)]$, was synthesized according to a published procedure (Diop et al., 2003) by mixing ethanolic solutions of oxalic acid dihydrate (0.150 g, 1.190 mmol) and triphenyltin hydroxide (0.874 g, 2.380 mmol).

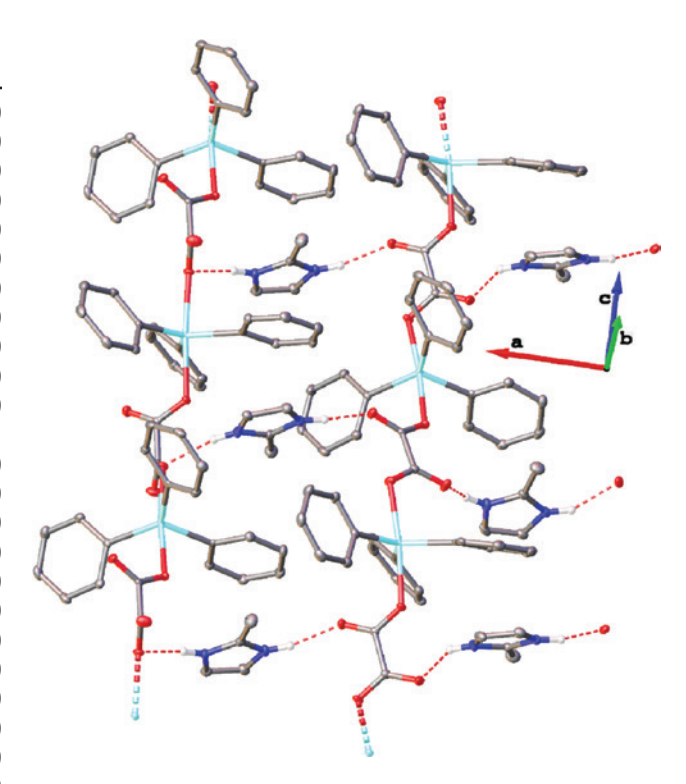


Figure 2: OLEX2 view showing the infinite chains of **1**. For clarity, only H atoms involved in hydrogen bonds are depicted. The origin of the coordinate system is arbitrary. Red and dotted line: hydrogen bonds; bicolored stipple cone: covalent bonds.

The title compound was finally obtained by reacting methanolic solutions of bis(triphenyltin) oxalate (0.388 g, 0.492 mmol, 35 mL CH₃OH) and bis(2-methyl-1H-imidazol-3-ium) oxalate (0.250 g, 0.984 mmol, 30 mL CH₃OH) at room temperature. After several days of a slow evaporation at room temperature, colorless crystals were collected from the clear solution (0.235 g, 92 yield %; mp >220°C (dec)). Suitable for an X-ray crystallographic structure determination, they were characterized as [C,H.N.][Ph,Sn(C,O,)].

'H-NMR (CD₃OD, 300 K): δ =2.55 (s, 3H, C H_3 , 2-methyl-1H-imidazol-3-ium), 7.29 (s, 2H, CH, 2-methyl-1H-imidazol-3-ium), 7.38 (m, 9H, CH, Ph), 7.73 (m, 6H, CH, Ph). IR (ATR, cm⁻¹): 3161 (w), 3068 (w), 2918 (w), 2720 (w), 1616 (s), 1594 (s), 1479 (m), 1424 (s), 1307 (m), 1286 (s), 1245 (s), 1160 (m), 1112 (m), 1048 (m), 1026 (m), 896 (m), 758 (s), 732 (s), 698 (s), 662 (s). Anal. Calcd. for C₂₄H₂₂N₂O₄Sn-1/2H₂O (530.16): C 54.37, H 4.37, N 5.28. Found: C 54.77; H 4.36; N 6.45.

X-ray crystallography

A colorless prism-shaped crystal with dimensions $0.25\times0.20\times0.08\,\mathrm{mm}$ of 1 was selected and used for data collection using a Bruker D8 Venture triumph Mo diffractometer equipped with an Oxford Cryosystems low-temperature apparatus operating at T=100 K. Data were measured using MoK_{α} radiation (λ =0.71073 Å). The total number of runs and images was based on the strategy calculation from the program APEX2 (Bruker, 2014). Cell parameters were retrieved and refined using the Saint Software (Bruker, 2014). Data reduction was performed using the Saint Software, which corrects for Lorentz polarization. The structure was solved by Direct Methods using the

SHELXT (Sheldrick, 2015a) structure solution program and refined by least squares using SHELXL (Sheldrick, 2015b) with the aid of OLEX2 program (Dolomanov et al., 2009). All nonhydrogen atoms were refined anisotropically. Hydrogen atom positions were calculated geometrically and refined using the riding model.

CCDC 1473073(1) contains the supplementary crystallographic data for this paper. These data can be obtained free of charge from the Cambridge Crystallographic Data Centre via www.ccdc.cam. ac.uk/data_request/cif.

Acknowledgments: The authors gratefully acknowledge the Cheikh Anta Diop University of Dakar (Senegal), the Centre National de la Recherche Scientifique (CNRS, France), and the University of Bourgogne Franche-Comté (Dijon, France). The authors also thank the anonymous reviewers for their helpful and relevant comments, which have contributed significantly to improve the content of this manuscript.

References

- Amir, M. K.; Khan, S.; Zia-ur-Rehman; Shah, A.; Butler, I. S. Anticancer activity of organotin(IV) carboxylates. Inorg. Chim. Acta 2014, 423, 14-25.
- Bruker V8.34A. APEX2 and SAINT, Bruker AXS Inc., Madison, WI, USA, 2014.
- Callear, S. K.; Hursthouse M. B.; Threlfall, T. L. A systematic study of the crystallisation products of a series of dicarboxylic acids with imidazole derivatives. CrystEngComm. 2010, 12, 898-908.
- Chandrasekhar, V.; Nagendran, S.; Baskar, V. Organotin assemblies containing Sn-O bonds. Coord. Chem. Rev. 2002, 235, 1-52.
- Davies, A. G. Organotin Chemistry, 2nd ed.; Wiley-VCH: Weinheim,
- Davies, A. G.; Gielen, M.; Pannell, K. H.; Tiekink, E. R. T. In Tin Chemistry, Fundamentals, Frontiers, and Applications; John Wiley & Sons Ltd: Chichester, UK, 2008.
- Devendra, R.; Edmonds, N. R.; Söhnel, T. Organotin carboxylate catalyst in urethane formation in a polar solvent: an experimental and computational study. RSC Adv. 2015, 5, 48935-48945.
- Diop, L.; Mahon, M. F.; Molloy, K. C.; Sidibe, M. Crystal structure of bis-(aquatrimethylstannyl)oxalate $[Me_3Sn(H_2O)]_2C_2O_4$. Main Group Met. Chem. 1997, 20, 649-654.
- Diop, L.; Mahieu, B.; Mahon, M. F.; Molloy, K. C.; Okio, K. Y. A. Bis(triphenyltin) oxalate. Appl. Organomet. Chem. 2003, 17, 881-882.
- Diop, M. B.; Diop, L.; Plasseraud, L.; Maris, T. Crystal structure of 2-methyl-1*H*-imidazol-3-ium aquatrichlorido(oxalato-κ²O¹,O²) stannate(IV). Acta Cryst. 2015, E71, 520-522.
- Diop, M. B.; Diop, L.; Plasseraud, L.; Maris, T. Crystal structure of bis(2-methyl-1H-imidazol-3-ium) dihydroxidobis(oxalato- κ^2 0¹,0²) stannate(IV) monohydrate. Acta Cryst. 2016, E72, 355-357.
- Dolomanov, O. V.; Bourhis, L. J.; Gildea, R. J.; Howard, J. A. K.; Puschmann, H. OLEX2: a complete structure solution, refinement and analysis program. J. Appl. Cryst. 2009, 42, 339-341.
- Gielen, M.; Biesemans, M.; Willem, R. Organotin compounds: from kinetics to stereochemistry and antitumour activities. Appl. Organomet. Chem. 2005, 19, 440-450.

- Gueye, N.; Diop, L.; Molloy, K. C.; Kociok-Köhn, G. Crystal structure of C₂O₄ (SnPh₃·dimethylformamide)₂. Main Group Met. Chem. **2011**, *34*, 3-4.
- Gueye, N.; Diop, L.; Molloy, K. C.; Kociok-Köhn, G. Dibenzylazanium (oxalato-k2O,O')triphenylstannate (IV). Acta Cryst. 2012, E68,
- Gueye, N.; Diop, L.; Stoeckli-Evans, H. Tetrakis(dipropylammonium) tetrakis(oxalato-κ²O¹,O²)stannate(IV) monohydrate: a complex with eight-coordinate Sn^{IV} atom. Acta Cryst. 2014, E70, m49-m50
- Hadjikakou, S. K.; Hadjiliadis, N. Antiproliferative and anti-tumor activity of organotin compounds. Coord. Chem. Rev. 2009, 253,
- Ivasenko, O.; Perepichka, D. F. Mastering fundamentals of supramolecular design with carboxylic acids. Common lessons from X-ray crystallography and scanning tunneling microscopy. Chem. Soc. Rev. 2011, 40, 191-206.
- Mao, W.; Bao, K.; Feng, Y.; Wang, Q.; Li, J., Fan, Z. Synthesis, crystal structure, and fungicidal activity of trioriganotin(IV) 1-methyl-1H-imidazole-4-carboxylates. Main Group Met. Chem. 2015, 38,
- Meneghetti, M. R.; Meneghetti, S. M. P. Sn(IV)-based organometallics as catalysts for the production of fatty acid alkyl esters. Catal. Sci. Technol. 2015, 5, 765-771.
- Ng, S. W.; Kumar Das, V. G.; Hossain, M. B.; Goerlitz, F.; Van Der Helm, D. Synthesis of triorganostannate esters of dicarboxylic acids. Crystal structure of bis(dicylohexylammonium) trioxalatotetrakis(tri-n-butylstannate)·2 ethanol. J. Organomet. Chem. 1990, 390, 19-28.
- Ng, S. W.; Kumar Das, V. G. Structural studies on triorganostannates derived from dicarboxylic acids. Crystal structure of tetramethylammonium oxalatotriphenylstannate bis(triphenyltin) oxalate. J. Organomet. Chem. 1993, 456, 175-179.
- Ng, S. W.; Kumar Das, V. G.; Luo B.-S.; Mak, T. C. W. Structural studies on oxalatotriorganostannates. Crystal structure of trimethylsulfonium catena-O-O'-oxalatotriphenylstannate. Z. Kristallogr. 1994, 209, 882-884.
- Sheldrick, G. M. SHELXT. Acta Cryst. 2015a, A71, 3-8.
- Sheldrick, G. M. SHELXL. Acta Cryst. 2015b, C71, 3-8.
- Sirajuddin, M.; Ali, S.; McKee, V.; Zaib, S.; Igbal, J. Organotin(IV) carboxylate derivatives as a new addition to anticancer and antileishmanial agents: design, physicochemical characterization and interaction with Salmon sperm DNA. RSC Adv. 2014, 4, 57505-57521.
- Sow, Y.; Diop, L.; Molloy, K. C.; Kociok-Köhn, G. Crystal and molecular structure of diorganoammonium oxalatotrimethylstannate, $[R_3NH_3][Me_3Sn(C_3O_4)]$ (R=i-Bu, cyclohexyl). Main Group Met. Chem. 2012, 34, 127-130.
- Tiekink, E. R. T. Structural chemistry of organotin carboxylates: a review of the crystallographic literature. Appl. Organomet. Chem. 1991, 5, 1-23.
- Tiekink, E. R. T. Steric Control Over Supramolecular Aggregation: A Design Element in Crystal Engineering? In Frontiers in Crystal Engineering. Tiekink, E. R. T. and Vittal J. J., Eds. John Wiley & Sons, Ltd: Chichester, 2006; chap. 6, pp. 117-134.

Supplemental Material: The online version of this article (DOI: 10.1515/mgmc-2016-0016) offers supplementary material, available to authorized users.